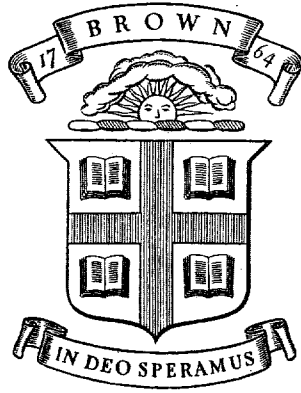


BU  
ARPA-E-75



Division of Engineering  
BROWN UNIVERSITY  
PROVIDENCE, R. I.

**SURFACE WAVES GUIDED BY A  
SLIT IN AN ELASTIC SOLID**

**L. B. FREUND**

TECHNICAL LIBRARY  
BLDG. 305  
ABERDEEN PROVING GROUND, MD.  
82047 TL

COUNTED 1

Advanced Research Projects Agency  
Department of Defense  
Contract SD-86  
Materials Research Program

**2006013017**

**ARPA E75**

**January 1971**

AD718372

2 copy  
1-TL  
1 - L. DeAngelis

UNITE - 2

SURFACE WAVES GUIDED BY A SLIT IN AN ELASTIC SOLID

L. B. Freund  
Assistant Professor of Engineering  
Brown University  
Providence, Rhode Island 02912

TECHNICAL LIBRARY  
BLDG. 305  
ABERDEEN PROVING GROUND, MD.  
STEAP-TL



## Abstract

Wave propagation in an isotropic elastic solid containing a slit is studied. The slit is viewed as an open crack of finite width and infinite length. In particular, the propagation of surface waves on the faces of the slit is considered. Making use of a reflection law for the oblique reflection of a Rayleigh wave from the tip of an open half plane crack, surface waves are superimposed to form guided surface waves in the slit. In order to carry out the construction of dispersion relations, an assumption on the rate of decay of body wave modes localized in the vicinity of the edges of the guide is made, and the range of validity of the assumption is discussed. The dispersion relations are obtained by geometrical construction, and representative dispersion curves are shown.

## Introduction

The subject of guided surface waves on elastic solids has been under study for several years. The main thrust for research in this area is the potential application of the theories to the design of electromechanical devices for electronic circuitry. For example, see the review article by White [1]. Of course, the results are also of interest in ultrasonics, geophysics, and other areas. Most work in the area has been directed toward determining the dispersion characteristics of various guiding configurations. A very thorough analysis of several configurations has been given by Tiersten [2], who modeled each surface waveguide by an appropriately selected system of membranes. Several other studies of the mechanical wave propagation process have appeared in the literature, but most are based on the work of [2]. See [1] for an extensive list of references. A method for studying the dispersion of guided surface waves was recently introduced [3] which is essentially a generalization of the scheme of superposition of plane waves for constructing guided waves. For any particular guide, the scheme assumes a knowledge of the law governing reflection of a surface wave from a discontinuity in boundary impedance resembling a single edge of the guide. The reflection problem must therefore be solved before guided waves can be constructed by superposition. The means of solution of this auxiliary problem is discussed in [3].

Nearly all surface waveguides which have been proposed are formed by modifying the plane surface of an elastic solid in some way. For example, a strip of relatively dense, elastically weak material may be deposited on the surface, or a relatively light, elastically stiff material may be deposited on the surface everywhere except along a strip. In any case, the general idea behind forming a surface waveguide on the surface of an elastic solid is to modify the surface in such a way as to make the surface wave speed inside the guide less

than the surface wave speed outside the guide. Since a heavy, weak film deposited on a surface decreases surface wave speed, and a light, stiff film increases surface wave speed [4], the two strip configurations mentioned above satisfy this condition.

The necessary condition for the existence of a surface waveguide may be generalized slightly. A strip of surface of an elastic solid will carry guided surface waves, without attenuation, if the surface wave speed in the guide is less than all other characteristic wave speeds of the configuration, including both body waves and surface waves. Clearly, this condition is satisfied by a slit (an open crack of finite width and infinite length) running through an elastic solid. That is, the speed of surface waves on the faces of the slit is less than all other characteristic speeds, namely, the body wave speeds. It is the purpose of this paper to determine the guiding characteristics of this slit waveguide configuration for the particular case of a homogeneous, isotropic elastic solid.

From the practical point of view, the slit configuration has several inherent advantages over other types of waveguides. Since it is made of a single material, fabrication of actual devices might be easier. Also, once the guide is constructed the air may be evacuated and the ends sealed to prevent atmospheric contamination and energy loss due to air-coupling.

Consider an unbounded isotropic elastic solid containing an open slit of constant width  $2d$  and indefinite length. Let  $x_j = (x, y, z)$  be a three-dimensional Cartesian coordinate system oriented so that the slit lies in the plane  $z = 0$ . The edges of the slit are parallel to the  $y$ -axis and are defined by the straight lines  $z = 0$ ,  $x = \pm d$ . In reality, if the faces of the slit are to be separated, the opening must be of finite extent in the  $z$ -direction.

It is assumed, however, that the dimension of the gap is negligibly small with respect to  $d$  so that the slit may be viewed as a planar crack.

In the absence of body forces, the equation governing the components of the displacement vector  $U_i(x,y,z,t) = (U,V,W)$  is

$$C_{ijkl} U_{k,jl} - \rho \ddot{U}_i = 0 \quad i = 1,2,3 \quad (1)$$

where  $\rho$  is mass density. For the isotropic material being considered here,  $C_{ijkl}$  may be expressed in terms of the Lamé constants  $\Lambda$  and  $\mu$  as

$$C_{ijkl} = \Lambda \delta_{ij} \delta_{kl} + \mu(\delta_{ik} \delta_{jl} + \delta_{il} \delta_{jk}) \quad (2)$$

The boundary conditions which must be satisfied on  $z = 0$  for the faces of the crack to be traction-free are

$$\Sigma_{i3}(x,y,0^\pm,t) = 0, \quad |x| < d, \quad i = 1,2,3 \quad (3)$$

where the notation  $0^\pm$  means that the stress components must vanish as  $z \rightarrow 0$  through positive or negative values. The stress matrix  $\Sigma_{ij}$  is related to the displacement components by

$$\Sigma_{ij} = C_{ijkl} U_{k,l} \quad (4)$$

The displacement is required to be continuous at all points of the solid and to have a unique finite limit at all points of the boundary, in particular, along the edges of the slit. The stress may be singular at the edges subject to the condition that the strain energy density be integrable there.

It is desired to study the characteristics of the slit configuration when it is viewed as a waveguide for surface waves. If the slit is to serve as a waveguide it must satisfy the condition that the average energy flux through

any cross section of the guide, due to passage of a time-harmonic wave, is a fixed constant. In general, the energy exists in the form of surface waves on both the  $z = 0^+$  and  $z = 0^-$  faces of the crack, and a continual exchange of energy takes place between the faces in such a way that the net energy is conserved, that is, such that the net energy flux is the same for all sections. It appears that a direct approach to the general problem in which the amount of energy transfer between faces varies along the guide in some unknown way is prohibitively complicated. Two particular problems may be considered, however, the results of which can be combined to yield results for the general problem. The two cases considered are guided waves for which the  $z$ -component of displacement is an even function of  $z$  and the case for which it is an odd function of  $z$ . The common attractive feature of these two cases is that the rate of energy transfer from the face  $z = 0^+$  to  $z = 0^-$  is exactly the same as the rate of transfer from  $z = 0^-$  to  $z = 0^+$ . This can be seen from symmetry arguments or directly from the subsequent analysis, along with the results of [5]. As pointed out in [5], a surface wave for a given material is completely characterized by a single component of surface displacement. Therefore, only the  $z$ -component of surface displacement enters into the following discussion.

A solution of the equations of elasticity satisfying the boundary conditions (3) is sought for wave motion in the slit waveguide in the form

$$W(x,y,0^+,t) = A(x) e^{i(\omega t - \xi y)} \quad (5)$$

where  $A(x)$  is the mode shape,  $\omega$  is the circular frequency, and  $\xi$  is the real wavenumber of the guided wave. The displacement on  $z = 0^-$  is given by

$$W(x,y,0^-,t) = \pm W(x,y,0^+,t) \quad , \quad (6)$$

the plus (minus) sign holding for the case in which  $W$  is an even (odd) function of  $z$ , which will henceforth be referred to as case E (case O). It is improbable that an exact solution of the form (5) can be found, and additional assumptions must be made to obtain approximate results for the problem. To this end, the following auxiliary problem is introduced.

#### The Associated Reflection Problem

In order to obtain approximate dispersion relations for the slit waveguide, the simpler problem of the oblique reflection of a Rayleigh surface wave from the tip of a half-plane crack is considered. This may be thought of as a special case of the slit configuration with one edge of the guide moved off to infinity.

Consider an unbounded homogeneous body of the same elastic material as above containing a semi-infinite crack. Cartesian coordinates are prescribed in the body in such a way that the crack occupies the half-plane  $z = 0, x < 0$ . The faces of the crack are taken to be traction-free. The motion of the solid is governed by (1), (2) and (4), which are now subject to the boundary conditions

$$\Sigma_{i3}(x,y,0^{\pm},t) = 0, \quad x < 0, \quad i = 1,2,3. \quad (7)$$

The excitation is taken in the form of a surface wave on the face of the crack  $z = 0^+$ . A steady-state situation is assumed to exist with the surface wave, harmonic in time with circular frequency  $\omega$ , obliquely incident on the edge of the crack at  $x = z = 0$ . The incident disturbance on  $z = 0^+$  is written as

$$(U_j)^{inc.} = A_j e^{i(\omega t - \alpha x - \beta y)} \quad (8)$$

where  $A_j$  is the amplitude, and  $\alpha$  and  $\beta$  are components of the surface

wavenumber vector. If  $\gamma$  is the wavenumber of Rayleigh waves, then  $\alpha = \gamma \cos \theta$  and  $\beta = \gamma \sin \theta$  where  $\theta$  is the angle of incidence, that is,  $\theta$  is the angle between the normal to the constant phase lines of (8) and the edge of the crack. It can be shown that  $A_1$  and  $A_2$  may be expressed in terms of  $A_3$  [5].

A solution for the amplitudes and phase angles of the reflected surface waves on  $z = 0^+$  and  $z = 0^-$ , due to the incident wave (8), is given in [5]. Assuming that the scattered field has the same harmonic time-dependence as the incident wave, and observing that the physical system is invariant with respect to translation in the  $y$ -direction makes it possible to write the dependence of any typical field variable  $\phi(x,y,z,t)$  on  $y$  in the explicit form

$$\phi(x,y,z,t) = \phi(x,z) e^{i(\omega t - \beta y)} . \quad (9)$$

The problem is thus reduced to the determination of the amplitudes, such as  $\phi(x,z)$ , in the  $x,z$ -plane. The solution is derived by making use of a three-dimensional displacement representation theorem due to deHoop [6] and by Laplace transform methods. The exact Laplace transform (over  $x$ ) of the complete displacement field can be obtained. As is usually the case in problems of this sort, however, the inversion process which must be executed to obtain the displacement itself is prohibitively complicated. Fortunately, the parts of the diffracted field representing the reflected surface waves on  $z = 0^\pm$  can be extracted. This is due to the fact that the reflected surface waves appear in the transformed solution as simple poles, and may therefore be obtained by the evaluation of the residues of these poles. This evaluation was carried out in [5] and some of the main results are outlined here.

The ratios of the amplitudes of the reflected surface waves to the amplitude of the incident wave versus angle of incidence  $\theta$  are shown in Fig. 2 for the

representative case of Poisson's ratio equal to 0.25. The dilatational wavenumber  $\kappa_a$ , the shear wavenumber  $\kappa_b$  and the surface wavenumber  $\gamma$  are then related by  $\kappa_b^2 = 3\kappa_a^2$  and  $\gamma^2 = 3.549 \kappa_a^2$ . Figure 3 shows the phase change experienced by the surface waves upon reflection. For  $0^\circ \leq \theta < 23.2^\circ$  the apparent wavenumber  $\beta$  of the incident surface wave along the edge of the crack is greater than the larger of the two wavenumbers for body waves, that is, the apparent wave speed of the incident along the edge is less than the slower body wave speed. Consequently, the only body wave modes which are excited are those which have an amplitude which decays with distance from the edge of the crack in all directions and which have a wavenumber vector which has a real component along the edge but an imaginary component normal to the edge. The modes are said to be localized and nonpropagating, in the sense that they do not carry energy away from the guide.

A parameter which is a convenient measure of the relative energy of a surface wave is the square of the magnitude of the z-component of surface displacement. Taking the energy of the incident wave to be unity, the relative energy of each of the reflected surface waves is shown in Fig. 4. The sum of the energies is also shown. It is clear from this figure that for  $\theta < 23.2^\circ$  all the energy transported to the edge of the crack by the incident wave is carried away by the reflected surface waves. When  $\beta < \kappa_b$ , however, the apparent signal speed along the edge is greater than the shear wave speed. Propagating shear wave modes are therefore excited, which carry energy away from the edge. It is clear from Fig. 4 that this is indeed the case. In order to have a "conservative" surface wave reflection process, the angle of incidence must be restricted by  $\beta > \kappa_b$ .

The results of Figs. 2 through 4 are directly applicable only for an incident surface wave on  $z = 0^+$ . Suppose instead that a surface wave is incident

at angle  $\theta$  on  $z = 0^-$  and, for definiteness, suppose the  $z$ -component of surface displacement of the incident wave is the same as for the original problem. Then, letting  $u_i$  and  $u_i^*$  be the amplitudes of the reflected surface waves in the original and modified problems, respectively, it can be shown that [5]

$$u_i^*(x, 0^+) = u_i(x, 0^+) . \quad (10)$$

Similarly, if the incident surface wave on  $z = 0^-$  is  $\pi$  radians out of phase with the incident wave of the original problem, then

$$u_i^{**}(x, 0^+) = -u_i(x, 0^+) , \quad (11)$$

where  $u_i^{**}$  is the amplitude of the reflected surface waves in the second modified problems. Relations (10) and (11) are quite useful in constructing dispersion relations.

#### Dispersion Relations for the Guide

The results introduced in the previous section are now used to construct dispersion relations for guided surface waves in the slit configuration. As stated before, exact dispersion relations cannot be derived from these results and additional assumptions must be made in order to obtain approximate results. The particular assumption which is introduced is based on the behavior of the body wave modes near the edge of the crack for the surface wave reflection problem discussed in the previous section. Whereas the reflected surface waves appear in the transformed solution as simple poles, the body waves appear in the form of branch line integrals [5], which are far too complicated to make evaluation possible. The form of these integrals for  $z = 0$ , however, makes them ideally suited for application of Laplace's method of asymptotic evaluation

for  $|x| \rightarrow \infty$  [7]. The dominant term resulting from this calculation is

$$u_j(x,0) \approx A_j K_j |\kappa_a x|^{-3/2} e^{-|\lambda_b x|}, \quad x \rightarrow -\infty \quad (12)$$

$$\lambda_b = (\gamma^2 \cos^2 \theta - \kappa_b^2)^{1/2}$$

where the repeated index does not imply summation. The quantity  $K_j$  depends on  $\theta$  and is typically between zero and one. Equation (12) is a reasonable approximation for values of  $|x|$  greater than five or six times  $1/\lambda_b$ .

In view of (12), it is now assumed that the guided surface waves in the slit may be constructed by superimposing solutions of the surface wave reflection problem, in much the same way as guided waves are constructed in the elementary theories by the method of superposition of plane waves. An equivalent assumption is that the body wave disturbance localized in the vicinity of either edge of the guide has negligible effect on the state of deformation at the other edge. The result of this assumption is that, if a straight-crested surface wave is incident on one edge of the slit, it is reflected as though the other edge was absent, that is, it is reflected according to the reflection law depicted by Figs. 2 and 3. It is clear that for a given value of  $d$  the assumption is reasonable for sufficiently large values of  $\omega$ . It will be shown in the next section that the lower bound of the range of values of  $\omega$  for which the assumption is reasonable is sufficiently small so as to include almost the entire range of values for which dispersion relations can be obtained.

The construction of approximate dispersion relations here is similar to the method of [3]. It essentially consists of the superposition of wave trains on the faces of the slit in such a way as to satisfy the appropriate boundary conditions and, at the same time, to fit into either case E or case O. For the time being, attention is limited to those propagation modes which fit into

case 0 and which are symmetric, that is,  $A(x) = A(-x)$ .

Consider two trains of harmonic surface waves propagating on the face  $z = 0^+$  of the slit with angles of incidence  $\theta$  and  $-\theta$  and with common frequency  $\omega$ . Since only free waves are being considered here, admissible values of  $\theta$  are restricted by the condition  $\beta > \kappa_b$ . Further, suppose the two waves have the same amplitude, say unity, and are such that their crests intersect on  $x = 0$ . A diagram of several lines of constant phase is shown in Fig. 5. For definiteness, the solid lines are taken to represent crests, the dot/dash lines to represent valleys, and the phase is assumed to increase in the direction opposite to the direction of propagation. Diagrams for both faces of the slit are shown as viewed in the direction of increasing  $z$ . A particular place (value of  $y$ ) locating the intersection of two crests on  $z = 0^+$  is marked off and, since only case 0 is being considered, the same place locates the intersection of two valleys on  $z = 0^-$ . A reference line representing zero phase may be selected arbitrarily, and this line is identified with a particular wave crest in Fig. 5.

The dashed lines on  $z = 0^+$  in Fig. 5 and the dotted lines on  $z = 0^-$  are reflected waves, which may be determined according to the reflection law which was derived in [5] and which is represented in Figs. 2 and 3. Suppose the amplitude and phase of the reflected wave on  $z = 0^+$  shown in Figs. 2 and 3 are denoted by functions  $P(\theta)$  and  $2\pi p(\theta)$ , respectively. Similarly, let the amplitude and phase on  $z = 0^-$  shown in Figs. 2 and 3 be  $Q(\theta)$  and  $2\pi q(\theta)$ . The phase and amplitude of the dashed line on  $z = 0^+$  are made up of two contributions, one being the reflection of the zero phase line propagating on  $z = 0^+$  and the other being the reflection of the  $\pi$  phase line propagating on  $z = 0^-$ . In view of (11), the amplitude and phase of the surface wave on the dashed line is

$$w(\text{dashed line}) = P(\theta) e^{2\pi i p(\theta)} - Q(\theta) e^{2\pi i q(\theta)}, \quad (13)$$

where the common factor  $\exp i(\omega t - \beta y)$  has been omitted. From Fig. 3 it can be seen that, in the range of interest,  $2\pi q(\theta) = 2\pi p(\theta) + \pi/2$ . The quantity (13) may therefore be simplified,

$$w = [P(\theta) - iQ(\theta)] e^{2\pi i p(\theta)}. \quad (14)$$

Writing the complex number in brackets in polar form, (14) becomes simply

$$w = e^{2\pi i m(\theta)}, \quad m(\theta) = p(\theta) - \frac{1}{2\pi} \tan^{-1} \left[ \frac{Q(\theta)}{P(\theta)} \right]. \quad (15)$$

The amplitude turns out to be unity because, as shown in Fig. 5,  $P^2(\theta) + Q^2(\theta) = 1$  in the range of interest. Since the dashed line is  $2\pi m$  radians out of phase with the solid line, the dashed line trails the solid line by a distance  $2\pi m/\gamma$ . That is, the dashed line trails the solid line by the fraction  $m(\theta)$  of a full wavelength  $2\pi/\gamma$ . An expression similar to (15) for the dotted line on  $z = 0^-$  may also be derived.

The dispersion relation for case 0 and symmetric waves is now obtained [3]. The simplest situation, when any cross section of the surface  $z = 0^+$  is cut by at most two crests, is considered first. The dispersion relation is obtained in parametric form, with parameter  $\theta$ , by combining two pieces of information. First, the wavelength of the guided wave  $\ell = 2\pi/\xi$  is the spatial period of the superimposed surface wave fields. A wavelength is indicated in Fig. 5, where the interval is determined by the intersection of crests on  $z = 0^+$  or the intersection of valleys on  $z = 0^-$ . Second, the phase velocity of the guided surface wave is the apparent speed at which the point of intersection of crests or valleys moves along the y-axis. Letting  $v$  denote the dimensionless phase velocity, defined as the ratio of phase velocity to surface wave velocity,

the two pieces of information may be expressed mathematically as

$$\ell = \frac{2d}{\cot \theta} + \frac{2\pi(1-m)}{\gamma \cos \theta} \quad , \quad (16)$$

$$v \cos \theta = 1 \quad (17)$$

Both (16) and (17) may be determined from the geometry of Fig. 5. The result of eliminating  $\theta$  between (16) and (17) is

$$\xi d = \frac{m\pi}{(v^2-1)^{1/2}} \quad , \quad (18)$$

where the relation  $\ell = 2\pi/\xi$  has been used. In (15),  $m$  was defined as a function of  $\theta$ . In view of (17),  $m$  may also be expressed as a function of  $v$ . Equation (18) is then the dispersion relation for the lowest symmetric mode, for case 0, of guided surface wave propagation in the slit.

Dispersion relations for the higher symmetric modes and for the antisymmetric modes, for case 0, are obtained in a similar way [3]. For the  $m$ th symmetric mode

$$\xi d = \frac{\pi(m+M-1)}{(v^2-1)^{1/2}} \quad , \quad m = 1,2,3 \dots \quad (19)$$

and for the  $L$ th antisymmetric mode

$$\xi d = \frac{\pi(m+L-1/2)}{(v^2-1)^{1/2}} \quad , \quad L = 1,2,3 \dots \quad (20)$$

The means of determining the corresponding mode shapes  $A(x)$  is discussed in [2,3].

Up to this point only case 0 has been considered. The derivation of dispersion relations for case E, however, proceeds in exactly the same way.

The part of Fig. 5 representing  $z = 0^+$  need not be modified for this case. The only difference is that, in view of (10), the phase and amplitude along the dashed line is given by

$$w(\text{dashed line}) = [P(\theta) + iQ(\theta)] e^{2\pi i p(\theta)}, \quad (21)$$

instead of by (14). The quantity (21) may be written as

$$w = e^{2\pi i n(\theta)}, \quad n(\theta) = p(\theta) + \frac{1}{2\pi} \tan^{-1} \left[ \frac{Q(\theta)}{P(\theta)} \right]. \quad (22)$$

The dispersion relations for case E are then given by (19) and (20) with  $m(v)$  replaced by  $n(v)$ .

### Discussion

Several dispersion curves for the slit waveguide are plotted in Fig. 6 for the case of Poisson's ratio of 0.25. For waves with wavelengths which are short with respect to the width of the slit, the phase velocity is very near the Rayleigh wave velocity. The curves for all modes are asymptotic to  $v = 1$  for  $\xi d \rightarrow \infty$ . As can be seen from the figure, each mode has a long wave cut-off wavenumber. For wavelengths which are greater than the cut-off wavelength free waves cannot exist. The cut-off wavenumber for each mode is determined as the wavenumber at which the phase velocity of the guided wave equals the shear wave velocity of the elastic solid. For wavenumbers below cut-off, or for phase velocities greater than the shear wave speed, shear wave modes are excited which carry energy away from the guide resulting in a decay of surface wave energy. Note that the cut-off wavenumbers for corresponding modes in case E and case 0 are different.

The group velocities of the various modes may also be calculated, as was done in [3]. It turns out that the group velocity is extremely close to the

phase velocity over almost the entire range of admissible wavenumbers.

With the introduction of the characteristic dimension  $d$  into the problem, the range of validity of the fundamental assumption employed in deriving dispersion relations can be investigated to a limited extent by considering the asymptotic forms of  $w$  as  $x \rightarrow 0^-$  and as  $x \rightarrow -\infty$  for the surface wave reflection problem discussed in the previous section. Only case 0 will be considered, with similar results holding for case E. That is, the particular reflection problem in which incident surface waves of common amplitude (say unity), frequency and angle of incidence propagate on  $z = 0^+$  and  $z = 0^-$ , but the waves are  $\pi$  radians out of phase, is considered. The net displacement is then constructed according to the scheme suggested by (11).

The net surface displacement  $w$ , for the case being considered, has the representation [5]

$$w(x, 0^\pm) = \pm \frac{1}{2\pi i} \int_{-i\infty}^{i\infty} \bar{w}(\lambda) e^{\lambda x} d\lambda, \quad (23)$$

which arises naturally from solution of the problem by integral transform methods. The relevant Tauberian theorem for Laplace transforms [8] states that

$$\lim_{x \rightarrow 0^-} \frac{w(x, 0)}{|x|^\nu} = \lim_{\lambda \rightarrow -\infty} \frac{(-\lambda)^{\nu+1} \bar{w}(\lambda)}{\Gamma(1+\nu)} \quad (24)$$

where  $\Gamma$  is the gamma function. Applying (24) to the explicit solution of the reflection problem [5] shows that

$$w(x, 0^\pm) = \pm C(\theta) |k_a x|^{1/2}, \quad x \rightarrow 0^- \quad (25)$$

The coefficient  $C(\theta)$  has been evaluated numerically for Poisson's ration of 0.25, and it is fit very closely over the full range of interest by the

parabola  $C(\theta) = 2.71 \theta^2$  where the angle of incidence  $\theta$  is measured in radians. The total  $w$  near  $x = 0$  is zero, because of the symmetry with respect to  $z = 0$ . The contribution to the total  $w$  due to body waves near  $x = 0$  may then be computed by subtracting the surface wave contribution from (25). Denoting the body wave contribution by  $w_b$  and omitting a common phase factor,

$$w_b(x, 0^+) = (2.71)\theta^2 |\kappa_a x|^{1/2} - [1 + \cos 2\pi m(\theta)] \quad (26)$$

as  $x \rightarrow 0^-$ . The term in brackets in (26) is the net contribution due to the incident and reflected surface waves on  $z = 0^+$ .

The integrand  $\bar{w}(\lambda)$  of (23) has a simple pole at a point determined by the surface wave speed, and branch points determined by the body wave speeds. For  $x < 0$  the path of integration may be deformed into the right half plane, yielding a representation for  $w$  in the form of a residue of a pole, representing surface waves, and a branch line integral, representing body waves. The form of the latter makes it well suited for application of Laplace's asymptotic method of evaluation [7] as  $x \rightarrow -\infty$ . As is indicated in (12), the result of this calculation is

$$|w_b(x, 0^+)| = K(\theta) |\kappa_a x|^{-3/2} e^{-|\lambda_b x|} \quad (27)$$

as  $x \rightarrow -\infty$ . The amplitude  $K(\theta)$  has been evaluated numerically for Poisson's ratio of 0.25, and it is closely fit over the full range of interest by the straight line  $K(\theta) = 1.86 \theta$  where  $\theta$  is measured in radians.

The result (26) then indicates how  $w_b$  varies as  $x$  decreases from zero, and (27) provides a bound for  $w_b$  for values of  $|\kappa_a x|$  much larger than unity. As an example, (26) and (27) are shown in Fig. 7 for the case of  $\theta = 15^\circ$ . The

parabola (26) is continued beyond  $|\kappa_a x| = 0.25$  as a dashed line merely to indicate a possible form of  $w_b$ . The important feature is that, as  $|\kappa_a x|$  becomes large with respect to unity,  $|w_b|$  is very small.

To see how the validity of the main assumption made in determining approximate dispersion relations may be studied, consider a particular point on the dispersion curve, for example,  $v = 1.035$  and  $\xi d = 4.798$ . From (17) it can be seen that this value of  $v$  corresponds to  $\theta = 15^\circ$ . For this point on the dispersion curve, the value of  $\kappa_a x$  may be determined for  $x = -2d$ . From the identity  $v = \gamma/\xi$  and the fact that  $\gamma^2 = 3.549 \kappa_a^2$ , it follows that

$$[|\kappa_a x|]_{x=-2d} = \frac{2v\xi d}{(3.549)^{1/2}} = 5.38 \quad .$$

Going back to Fig. 7, it can be seen that for  $|\kappa_a x| = 5.38$  the value of  $w_b$  is bounded by  $|w_b| < 0.010$ . That is, the magnitude of the body waves is less than about 1% of the magnitude of surface waves. As  $\theta$  becomes larger the error increases, and as  $\theta$  becomes smaller the error decreases.

As was remarked earlier, cases E and O may be combined by specifying appropriate amplitudes to represent any guided wave in the slit. Because these two cases have different wavenumbers for a given phase velocity  $v$ , a wave resulting from the superposition of the two cases will exhibit the interesting phenomenon of beats. Consider the simplest situation in which the two cases have a common amplitude and the new guided wave is formed by subtracting the lowest symmetric mode of case E from the lowest symmetric mode of case O. Then, at regularly spaced values of  $y$ , the net displacement on the faces of the slit will be zero. The usual analysis of the intermittent vibration phenomenon leads to the result that the spacing of these zeros is

$$\Delta y/d = 2\pi/|(\xi d)_E - (\xi d)_O|$$

where the subscripts  $E$  and  $O$  denote values of dimensionless wavenumber of cases  $E$  and  $O$  at a given phase velocity  $v$ . For example, for  $v = 1.035$  the spacing of the zeros is about  $\Delta y/d \approx 8$ . At any given station on either face of the slit, of course, the period of the beat is exactly the time it takes for the wave to travel a distance  $\Delta y$ .

#### Acknowledgment

The research support of the Advanced Research Projects Agency, Department of Defense, through Brown University is gratefully acknowledged.

References

1. White, R. M., "Surface Elastic Waves," Proceedings of the IEEE, Vol. 58, 1970, pp. 1238-1276.
2. Tiersten, H. F., "Elastic Surface Waves Guided by Thin Films," Journal of Applied Physics, Vol. 40, 1969, pp. 770-789.
3. Freund, L. B., "Guided Surface Waves on an Elastic Half Space," Journal of Applied Mechanics, to appear.
4. Achenbach, J. D., and Keshava, S. P., "Free Waves in a Plate Supported by a Semi-Infinite Continuum," Journal of Applied Mechanics, Vol. 34, 1967, pp. 397-404.
5. Freund, L. B., "The Oblique Reflection of a Rayleigh Wave from a Crack Tip," submitted for publication.
6. deHoop, A. T., "Representation Theorems for the Displacement in an Elastic Solid," D.Sc. thesis, Technische Hogeschool, Delft, 1958.
7. deBruijn, W. G., Asymptotic Methods in Analysis, North-Holland, Amsterdam, 1961, Chapter 4.
8. van der Pol, B. and Bremmer, H., Operational Calculus, Cambridge, 1964, Chapter 7.

Figure Captions

- Fig. 1. The slit viewed along the negative y-axis.
- Fig. 2. The reflection coefficient versus angle of incidence for the associated reflection problem.
- Fig. 3. The phase change versus angle of incidence for the associated reflection problem.
- Fig. 4. Relative surface wave energies versus angle of incidence for the associated reflection problem.
- Fig. 5. Diagrams used to determine dispersion relations.
- Fig. 6. Dispersion curves for first and second symmetric modes and first antisymmetric mode, for both case E (dashed) and case O (solid).
- Fig. 7. Bounds on body wave displacement on  $z = 0$  for large  $|\kappa_a x|$ , case O.

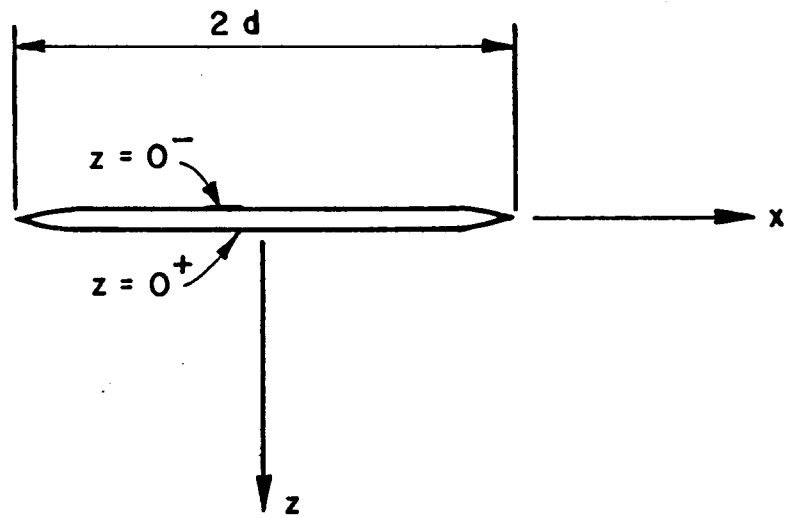


FIGURE I

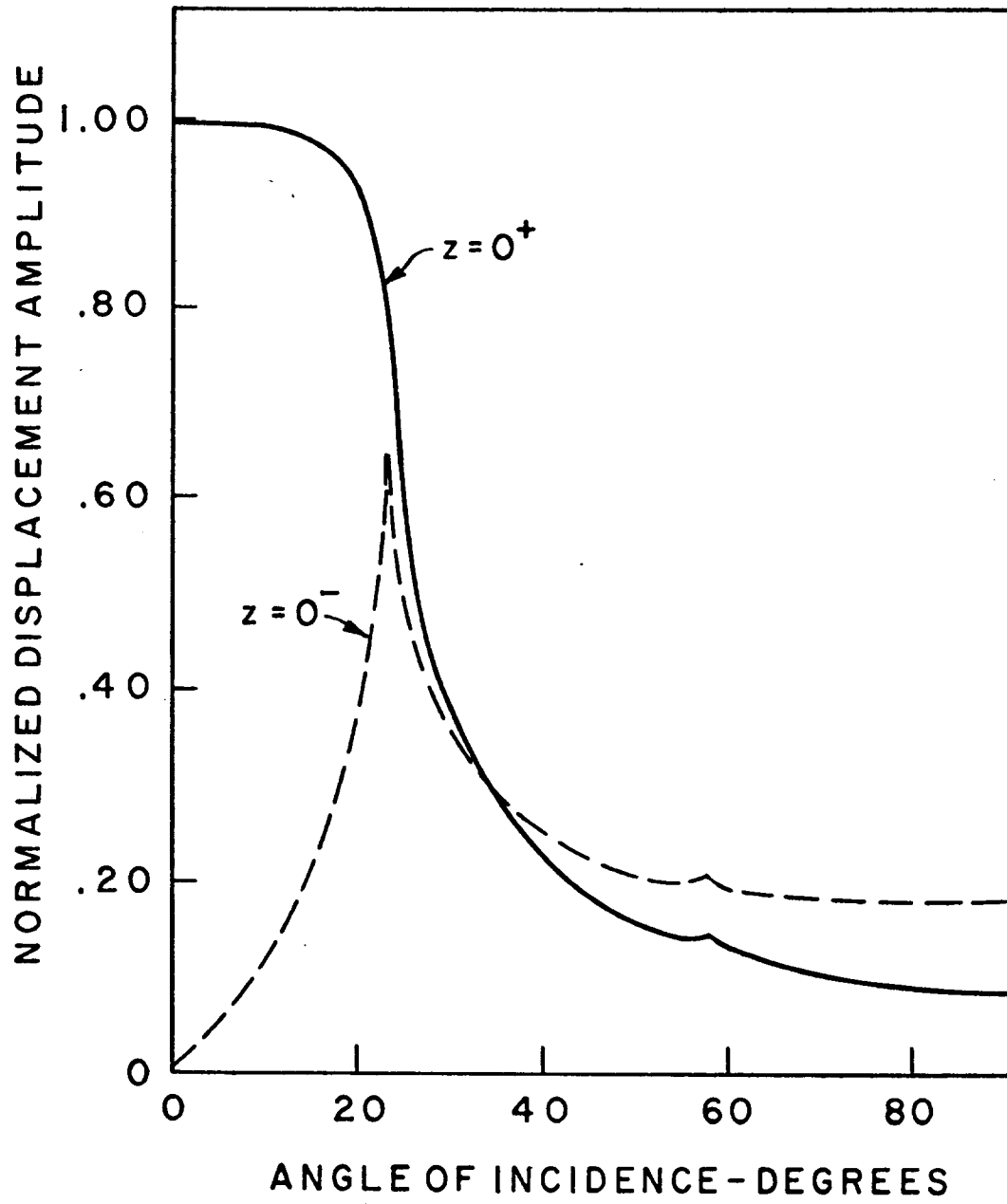


FIGURE 2

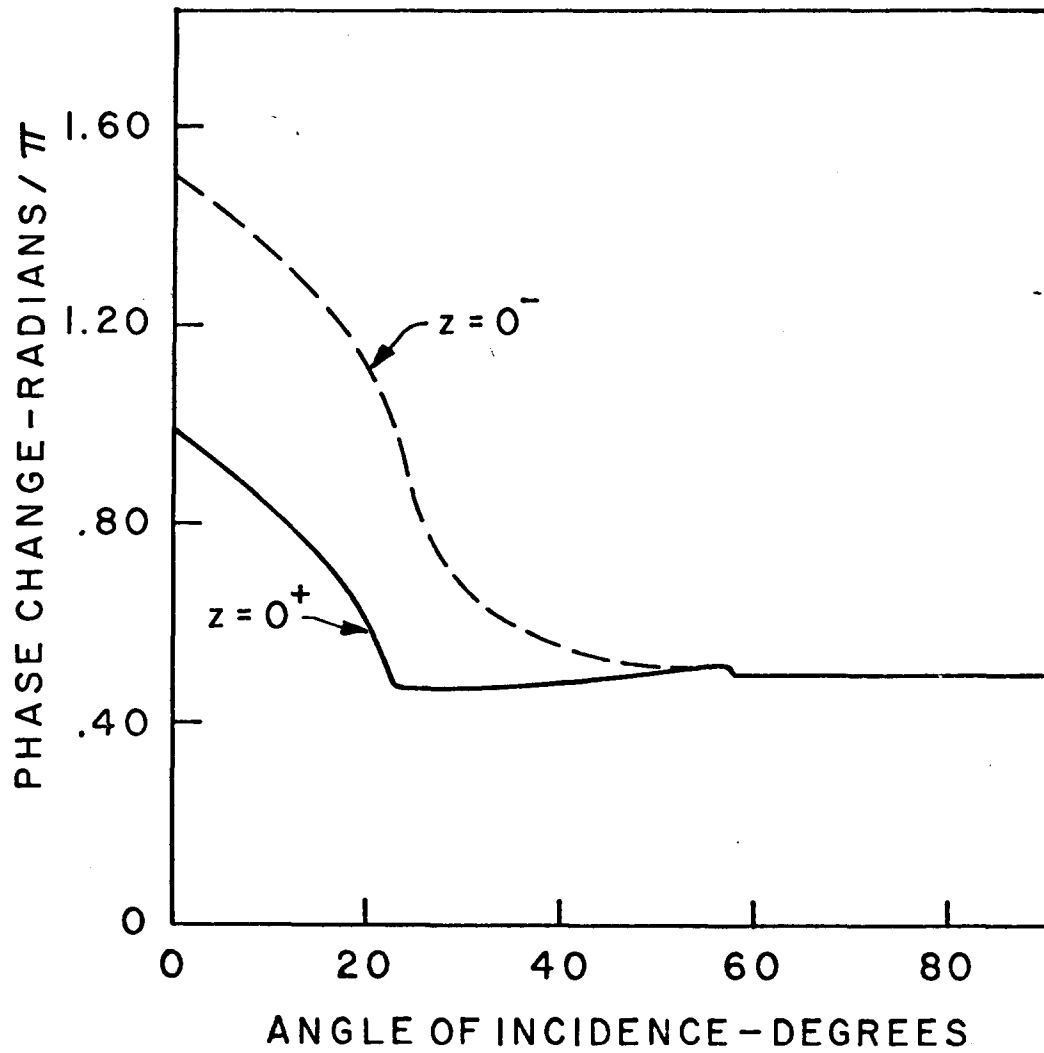


FIGURE 3

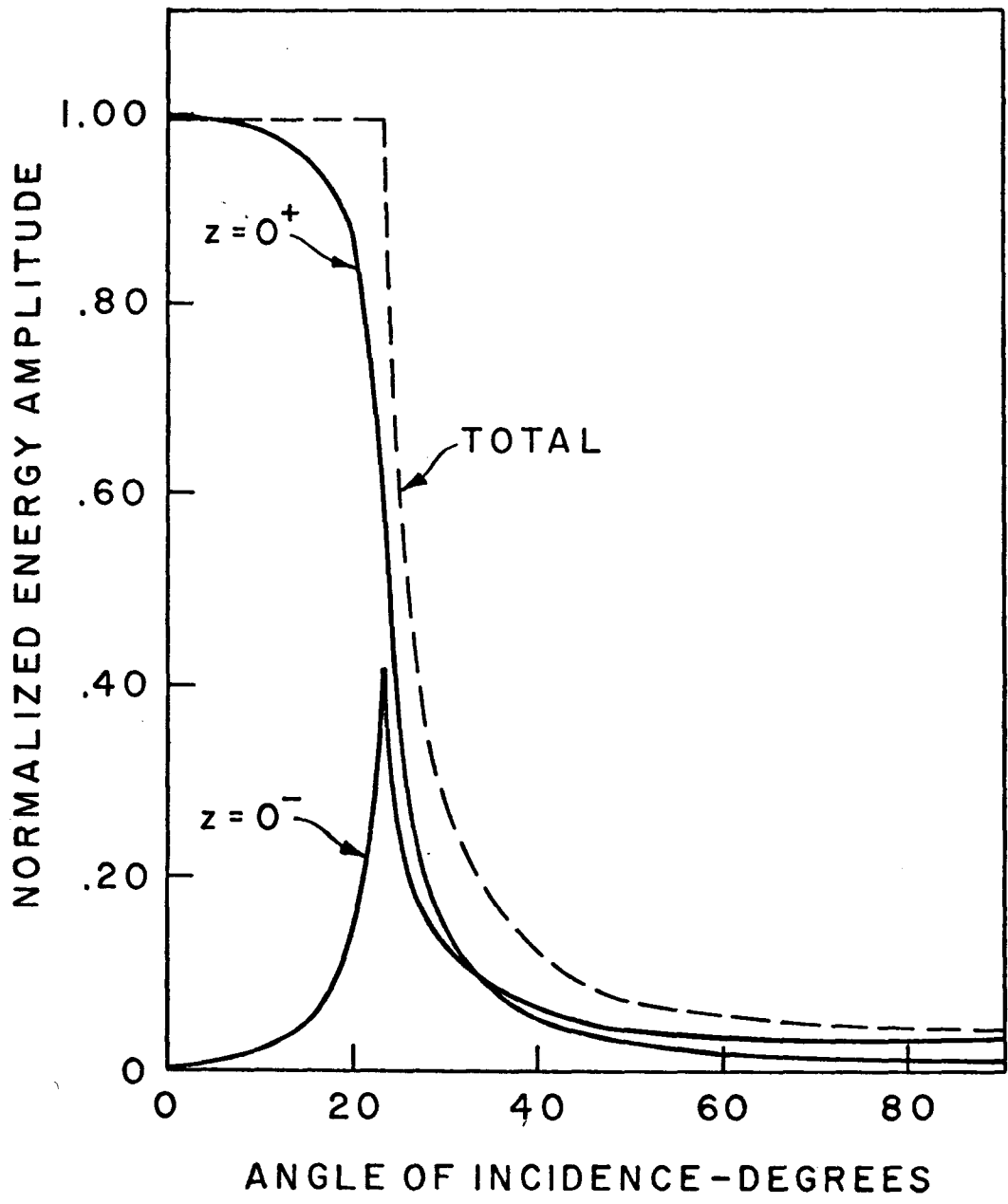


FIGURE 4

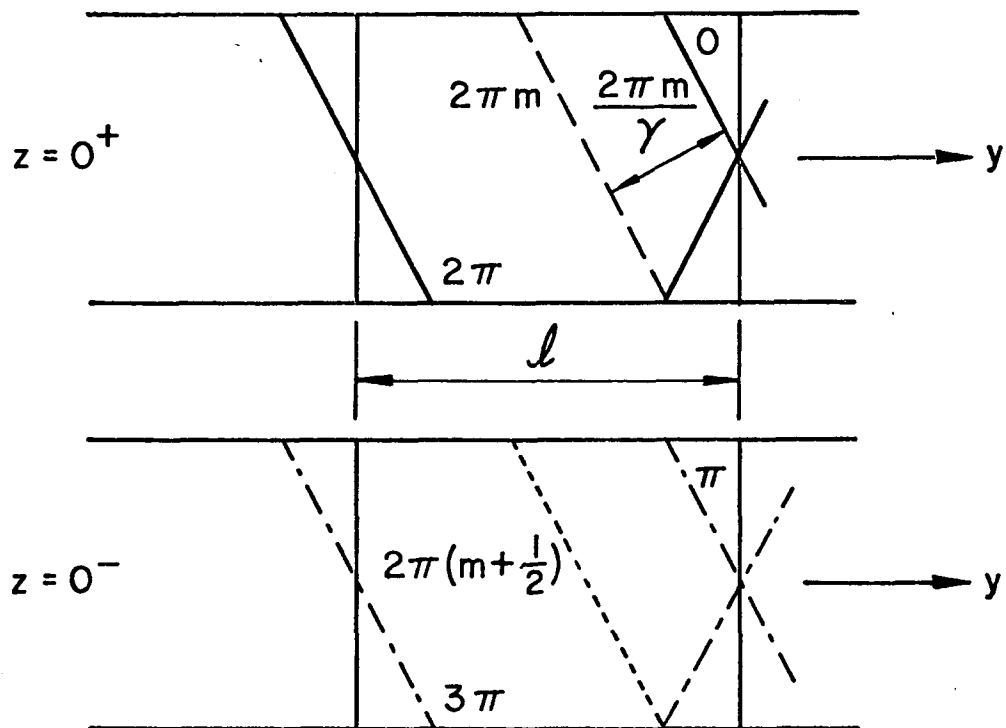


FIGURE 5

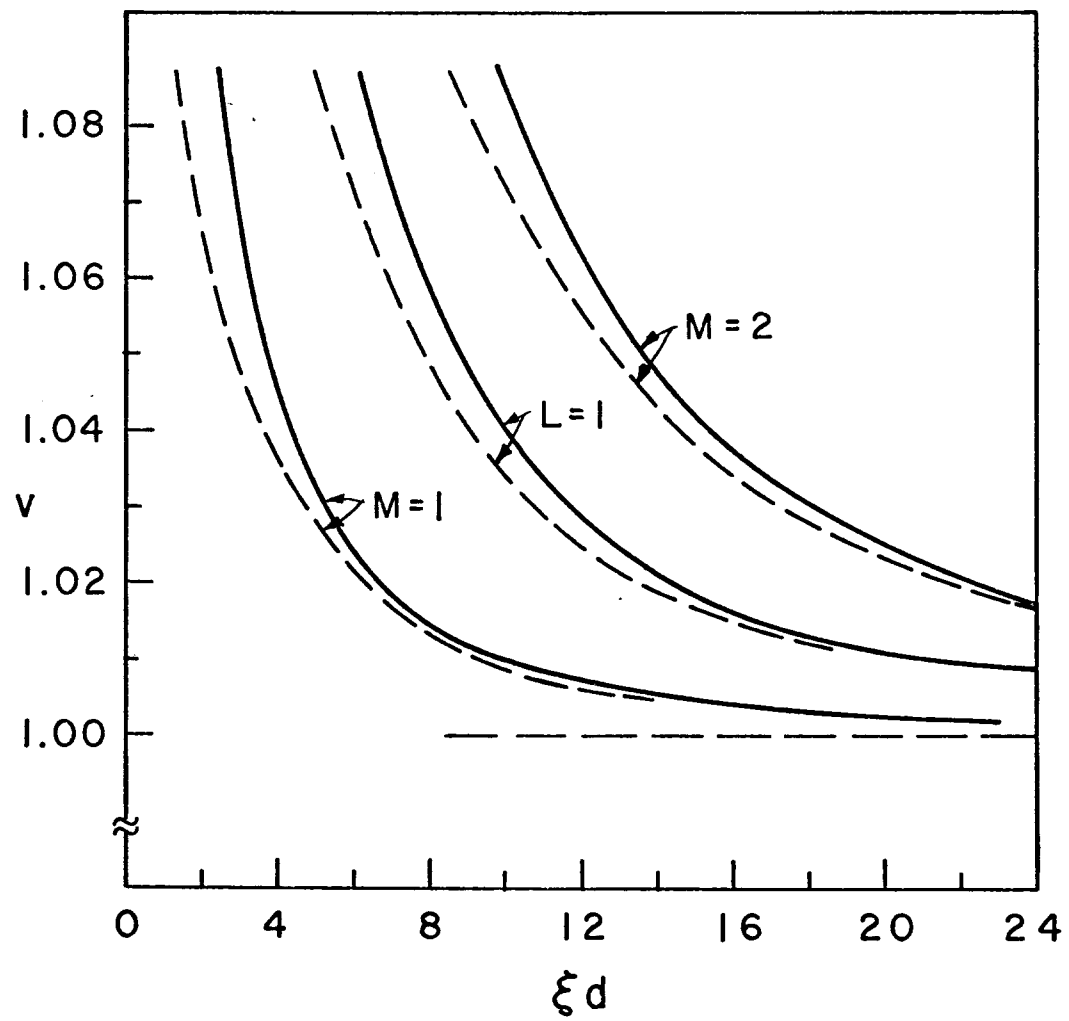


FIGURE 6

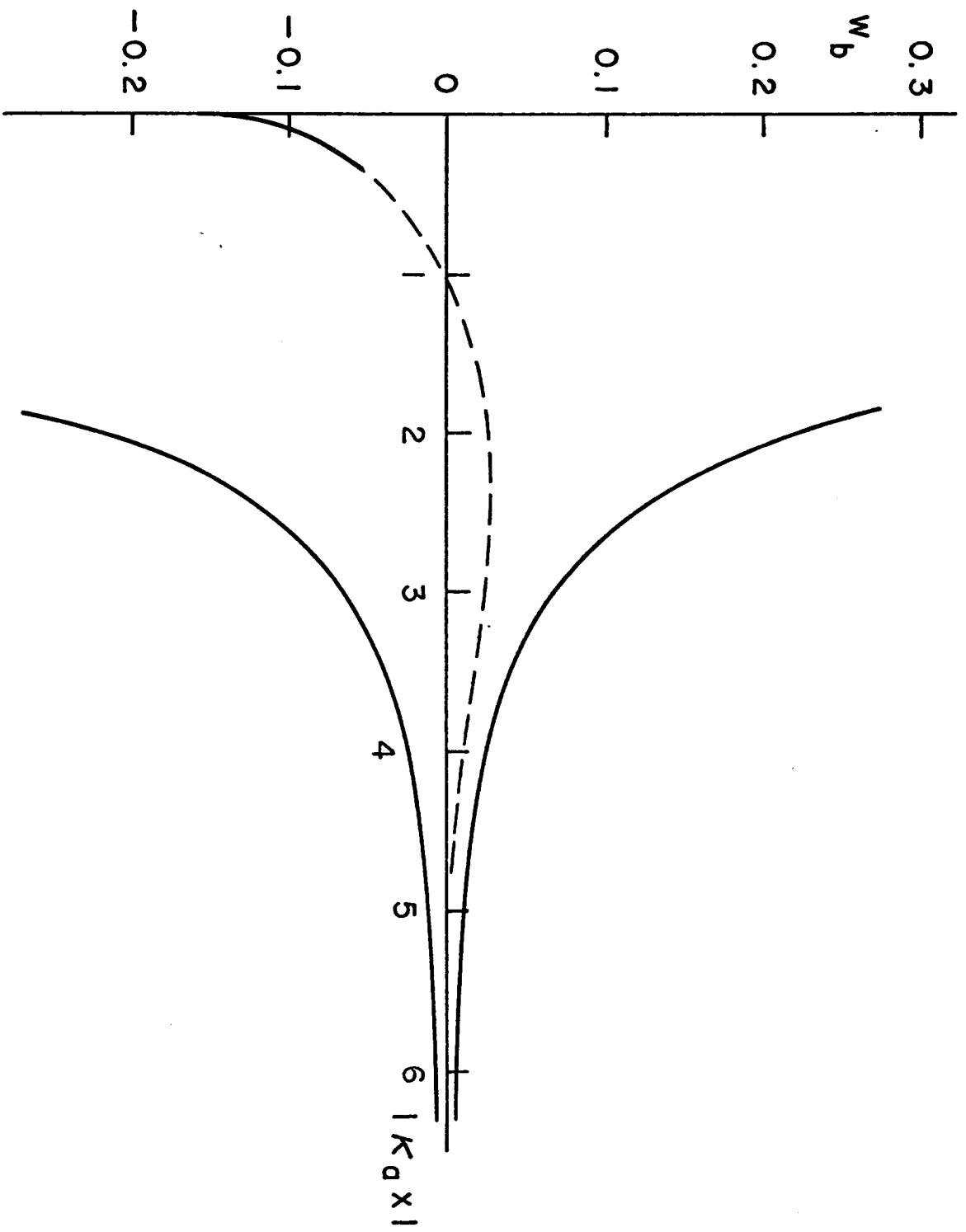


FIGURE 7